Langmuir

Article

pubs.acs.org/Langmuir

Protein Recognition by a Self-Assembled Deep Cavitand Monolayer on a Gold Substrate

Ying Liu,[†] Toshiaki Taira,[‡] Michael C. Young,[†] Dariush Ajami,[‡] Julius Rebek, Jr.,*[,‡] Quan Cheng,*[,†] and Richard J. Hooley*[,†]

[†]Department of Chemistry, University of California, Riverside, Riverside, California 92521, United States

[‡]The Skaggs Institute for Chemical Biology and the Department of Chemistry, The Scripps Research Institute, 10550 North Torrey Pines Road, La Jolla, California 92037, United States

Supporting Information

ABSTRACT: This paper details the first use of a self-folding deep cavitand on a gold surface. A sulfide-footed deep, self-folding cavitand has been synthesized, and its attachment to a cleaned gold surface studied by electrochemical and SPR methods. Complete monolayer formation is possible if the cavitand folding is templated by noncovalent binding of choline or by addition of space-filling thiols to cover any gaps in the cavitand adsorption layer. The cavitand is capable of binding trimethylammonium-tagged guests from an aqueous medium and can be deposited in 2 × 2 microarrays on the surface for characterization by SPR imaging techniques. When biotin-labeled guests are used, the cavitand:guest construct can recognize and immobilize streptavidin proteins from aqueous solution, acting as an effective supramolecular biosensor for monitoring protein recognition.

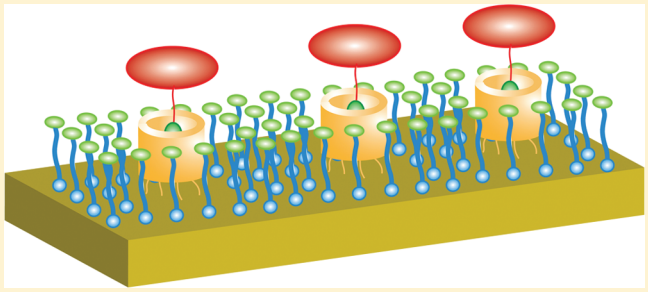

INTRODUCTION

The incorporation of synthetic host molecules on a defined substrate surface has been a goal of chemists for many years. By attaching well-known host molecules such as calixarenes, shallow cavitands, and cyclodextrins to a gold or silica surface, detection of small molecules is possible.[1] Many of these molecules are commercially available, and their ease of derivatization and surface attachment is an obvious attraction. They have been tested for self-assembly[2] and the detection of a range of small molecules including gas vapors,[3] polycyclic aromatic hydrocarbons via surface-enhanced Raman spectroscopy (SERS)[4] and adrenaline and catecholamine via electrochemistry.[5] More recently, improved vapor sensing has been shown with phosphonate cavitands that show much higher binding affinities for charged substrates than calixarenes or Cram-type cavitands.[6] These hosts, however, display rather small binding pockets, and this leads to two challenges: recognition of larger and/or more flexible guests is difficult and solvent competition can be problematic. Solvents such as chloroform are present at vastly higher concentrations than the target guests, and so binding of solvent must be outcompeted. One solution to this problem is multivalency: by adding substrates that can coordinate to multiple surface-bound species,[7] a variety of strongly bound substrates can be attached to surfaces, allowing for nanofabrication[8] and the sensing and immobilization of biomolecules.[9]

While the field of surface attachment has focused on shallow, well-precedented hosts, significant advances have been made in the synthesis of solution-phase host species.[10] Deep cavitands are bowl-shaped molecules that feature sizable concave surfaces.[11] By appending flexible walls to the rim of the resorcinarene framework, larger cavities are possible at the cost of multiple conformations.[12] Appending secondary amides[13] or benzimidazoles[14−16] along the periphery stabilizes the "vase-like" structure shown in Figure 1 by intramolecular hydrogen bonding.[17] These deep cavitands show wide-ranging properties, from molecular recognition[18] to catalysis[19] and selective stabilization of reactive intermediates.[20,21] Surface attachment of deep cavitands can provide a number of advantages over smaller, shallow hosts such as derivatized cyclodextrins and calixarenes.[3,7−9] Real-time analysis of guest binding from an aqueous medium is possible rather than detection of small organics through vapor absorption, and selective target immobilization is possible through both size/shape and charge-based noncovalent interactions.

Unfortunately, there are synthetic challenges in the formation of deep cavitands with suitable groups for surface attachment, so their use in surface chemistry has been limited. Here we describe the synthesis of a self-folding deep cavitand with thioether feet and its attachment to a gold surface. The surface coverage and guest binding properties are characterized by electrochemistry, surface plasmon resonance (SPR) spectroscopy and SPR imaging.

Received: October 7, 2011
Revised: December 7, 2011
Published: December 10, 2011

   dx.doi.org/10.1021/la2039398 | *Langmuir* 2012, 28, 1391−1398

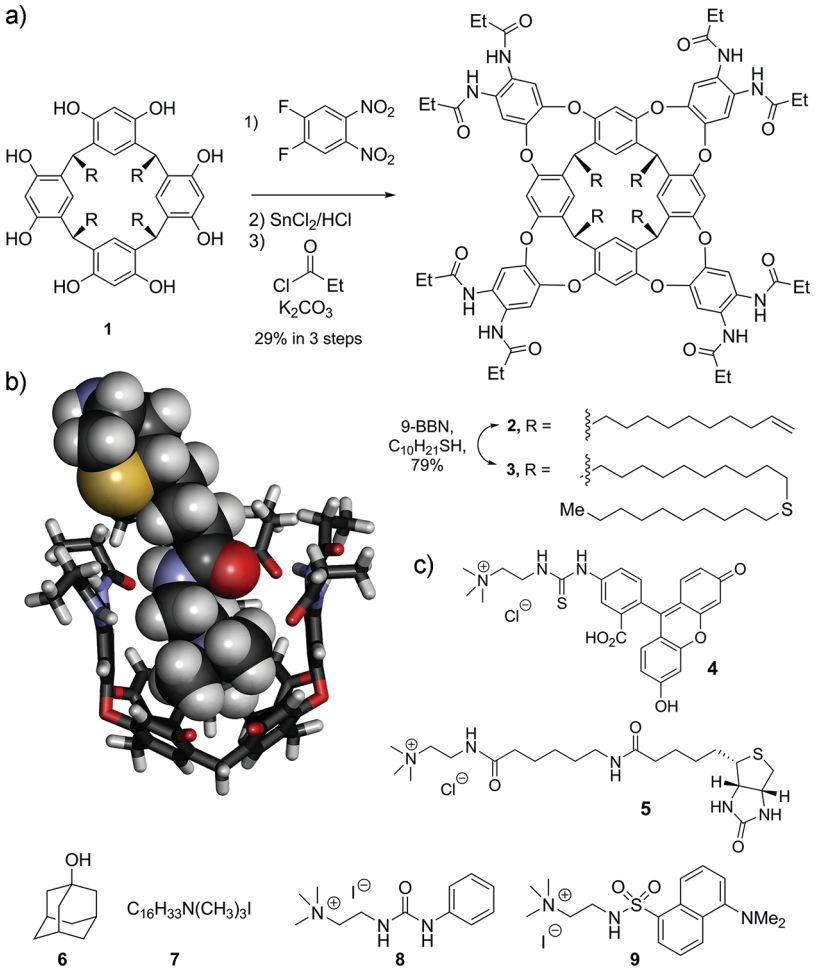

Figure 1. (a) Synthesis of cavitands **1**–**3**. (b) Minimized conformation of **1** (SPARTAN, AM1 forcefield) with a NMe_3^+-tagged guest in the cavity; (c) the guests **4**–**9** used in this study.

EXPERIMENTAL SECTION

^{1}H spectra were recorded on a Varian Inova 400 or a Bruker DRX-600 spectrometer with a 5-mm QNP probe. Proton (^{1}H) chemical shifts are reported in parts per million (δ) with respect to tetramethylsilane (TMS, δ = 0), and referenced internally with respect to the protio solvent impurity. Deuterated NMR solvents were obtained from Cambridge Isotope Laboratories, Inc., Andover, MA, and used without further purification. All other materials were obtained from Aldrich Chemical Co., St. Louis, MO and were used as received. Solvents were dried through a commercial solvent purification system (SG Water, Inc.). Cyclic voltammetric experiments were performed on a CHI 650A Electrochemical Workstation (CH Instruments Inc.). A dual channel SPR spectrometer NanoSPR-321 (NanoSPR, Addison, IL) with a GaAs semiconductor laser light source (λ = 670 nm) was used for all SPR measurements. Fluorescence microscopy was carried out on a Zeiss LSM 510 confocal laser scanning microscope with 488 nm argon laser excitation and a CCD camera. The synthesis of resorcinarene **1**[22] and guests **4** and **5**[23] was performed according to literature precedent.

Octaamide Cavitand 2. (1) To a solution of resorcinarene **1** (6.0 g, 4.3 mmol) and difluorodinitrobenzene (4.8 g, 23.6 mmol) in DMF (180 mL) was added Et_3N (12.6 mL, 90.6 mmol) at 0 °C. The solution was heated at 70 °C and stirred for 24 h. The resulting mixture was poured into 1.5 L of water containing 2 M HCl (30 mL) and the precipitate was collected by filtration and washed with water. The product was extracted with EtOAc and dried with $MgSO_4$. Evaporation of the solvent gave crude octanitrocavitand as a brown solid (13.6 g). This compound was used for next reaction without further purification.

(2) To a solution of octanitro cavitand (3.0 g) in ethanol (80 mL) and concentrated HCl (20 mL) was added tin(II) chloride dihydrate (23 g, 102 mmol). The mixture was stirred at 70 °C for 22 h and then allowed to evaporate in vacuo to give the crude octaamine cavitand. This compound was used for next reaction without further purification.

(3) To a solution of octamine cavitand in EtOAc (400 mL) was slowly added an aqueous solution (300 mL) of K_2CO_3 (51 g, 369 mmol) and propionyl chloride (20 mL, 229 mmol) at room temperature. The reaction mixture was stirred at room temperature for 2 h. The precipitate was filtrated and washed with EtOAc. The filtrate was dried with Na_2SO_4 and evaporated to give a crude product. Flash chromatography (SiO_2, hexane/EtOAc = 2:2, R_f = 0.34) afforded octaamide cavitand **2** (697 mg, 0.37 mmol, 29% in 3 steps) as a white solid. ^{1}H NMR (600 MHz, acetone-d_6) δ 9.48 (s, 8H, NH), 7.89 (s, 4H, ArH), 7.70 (s, 8H, ArH), 7.48 (s, 4H, ArH), 5.78–5.86 (8H, Ar*CH* and *CH*=CH_2), 5.00 (dd, 4H, J = 17.2, 1.6 Hz, *cis*-CH=CH_2), 4.92 (dd, 4H, J = 10.2, 1.0, *trans*-CH=CH_2), 2.52 (m, 8H, ArCHCH_2), 2.42 (m, 16H, COCH_2), 2.06 (m, 8H, CH_2CH=CH_2), 1.28–1.50 (48H, CH_2), 1.22 (t, 24H, J = 7.6 Hz, CH_3); ^{13}C{^{1}H}NMR (150 MHz, acetone-d_6) δ 174.3(C=O), 155.7 (aromatic), 150.3 (aromatic), 139.8 (*CH*=CH_2), 136.9 (aromatic), 129.4 (aromatic), 125.8 (aromatic), 121.7 (aromatic), 117.0 (aromatic), 114.7 (CH=*CH_2*), 34.5 (CH_2), 34.4 (CH_2), 32.9 (CH_2), 31.3 (CH_2), 30.5 (CH_2), 30.4 (CH_2), 30.3 (CH_2), 29.9 (CH_2), 29.8 (CH_2), 10.6 (CH_3); HRMS (ESI-TOFMS: MH^+) calcd. for $C_{116}H_{145}N_8O_{16}^+$ 1906.0773, found 1906.0731.

Sulfide-Footed Deep Cavitand 3. 9-Borabicyclo[3.3.1]nonane (9-BBN) (1.2 mL, 0.6 mmol, 0.5 M in THF solution) and 1-

dx.doi.org/10.1021/la2039398 | *Langmuir* 2012, 28, 1391–1398

decanethiol (1.1 mL, 5.3 mmol) were added to a solution of **2** (550 mg, 0.29 mmol) in THF (100 mL) at 0 °C. The solution was stirred at ambient temperature for 23 h. After evaporation of the solvent under reduced pressure, the crude product was extracted with hexane to give a sulfide-footed octaamido cavitand **3** as white solid (604 mg, 0.23 mmol, 79%). ^{1}H NMR (600 MHz, acetone-d_6) δ 9.48 (s, 8H, NH), 7.90 (s, 4H, ArH), 7.71 (s, 8H, ArH), 7.49 (s, 4H, ArH), 5.84 (4H, ArC*H*), 2.52 (24H, SCH_2, ArCHCH_2), 2.42 (m, 16H, COCH_2), 1.58 (m, 16H, SCH$_2CH_2$), 1.28−1.50 (48H, CH_2), 1.22 (t, 24H, J = 7.6 Hz, CH_3), 0.89 (t, 16H, J = 7.0 Hz, CH_3); ^{13}C{^{1}H}NMR (150 MHz, acetone-d_6) δ 174.3 (C═O), 155.7 (aromatic), 150.3 (aromatic), 136.9 (aromatic), 129.4 (aromatic), 125.8 (aromatic), 121.7 (aromatic), 117.1 (aromatic), 34.5 (CH_2), 33.0 (CH_2), 32.7 ($2CH_2$), 31.3 (CH_2), 30.6 ($2CH_2$), 30.5 (CH_2), 30.4 (CH_2), 30.1 ($2CH_2$), 29.7 (CH_2), 29.6 (CH_2), 29.0 (CH_2), 27.9 (CH_2), 27.7 (CH_2), 27.5 (CH_2), 27.2 (CH_2), 23.4 (CH_2), 22.9 (CH_2), 14.5 (CH_2), 10.6 (CH_3); MS (MALDI-TOFMS: MNa$^+$) calcd. for $C_{156}H_{232}N_8O_{16}S_4^+$ 2624, found 2625.

2-(Phenylureidoethyl)-trimethylammonium Iodide 8. 1-[2-(Dimethylamino)ethyl]-3-phenylurea[24] (100 mg, 0.48 mmol) was added to anhydrous THF (10 mL) followed by iodomethane (30 μL, 0.48 mmol). The mixture was heated in a sealed tube at 70 °C for 24 h, and subsequently cooled to ambient temperature. The solvent was evaporated in vacuo to give a yellow oil that was exposed to high vacuum for 48 h at 50 °C to afford a pale yellow solid (139 mg, 82%). ^{1}H NMR (400 MHz; D_2O) δ 7.42 (t, J = 8.3 Hz, 2H), 7.35 (d, J = 8.3 Hz, 2H), 7.20 (t, J = 8.3 Hz, 1H), 3.67 (q, J = 7.5 Hz, 2H), 3.47 (t, J = 7.5 Hz, 2H), 3.19 (s, 9H).^{13}C NMR (100 MHz; D_2O) δ 158.0, 138.3, 129.8, 124.7, 121.7, 65.4, 54.0, 34.6. (ESI) m/z calcd for $C_{12}H_{20}N_3O$ (M$^+$) 222.1595, found 222.1611.

2-(5-(Dimethylamino)naphthalene-1-sulfonamidoethyl)-trimethylammonium Iodide 9. (1) *Unsym*-dimethylethylenediamine (50 μL, 0.46 mmol) was added to a solution of dansyl chloride (124 mg, 0.46 mmol) in CH_3CN (10 mL). The reaction was stirred at 70 °C for 1 h before cooling, and the solvent was removed in vacuo to give *N*-2-dimethylaminoethyl-5-dimethylamino-naphthalene-1-sulfonamide monohydrochloride as a yellow-green oil, (160 mg, 97%). ^{1}H NMR (400 MHz; $CDCl_3$) δ 8.47 (d, J = 8.3 Hz, 1H), 8.31 (d, J = 8.3 Hz, 1H), 8.13 (d, J = 7.6 Hz, 1H), 7.97 (br, 1H), 7.49 (t, J = 8.3 Hz, 1H), 7.43 (t, J = 7.6 Hz, 1H), 7.10 (d, J = 7.6 Hz, 1H), 3.25 (br, 4H), 2.82 (s, 6H), 2.79 (s, 6H). ^{13}C NMR (100 MHz; $CDCl_3$) δ 151.7, 134.3, 130.6, 129.8, 129.4, 128.7, 123.3, 119.2, 115.5, 57.3, 45.5, 43.5, 38.1. (ESI) m/z calcd for $C_8H_{12}N_2O_2$ ([M+H]$^+$) 322.1505, found 322.1725.

(2) *N*-2-Dimethylaminoethyl-5-dimethylamino-naphthalene-1-sulfonamide monohydrochloride (160 mg, 0.45 mmol) was added to dichloromethane (20 mL) and subsequently washed with 6 M NaOH (2 × 20 mL). The combined aqueous layers were extracted with dichloromethane (10 × 10 mL). The combined organic phases were dried over $MgSO_4$, followed by evaporation in vacuo to yield the free amine as a yellow-green oil (100 mg, 65%) which was used without further purification in the next step. ^{1}H NMR (400 MHz; $CDCl_3$) δ 8.51 (d, J = 8.3 Hz, 1H), 8.29 (d, J = 8.3 Hz, 1H), 8.24 (d, J = 7.7 Hz, 1H), 7.54 (t, J = 8.3 Hz, 1H), 7.49 (t, J = 7.7 Hz, 1H), 7.15 (d, J = 7.7 Hz, 1H), 2.86 (t, J = 5.7 Hz, 2H), 2.85 (s, 6H), 2.12 (t, J = 5.7 Hz, 2H), 1.86 (s, 6H). ^{13}C NMR (100 MHz, $CDCl_3$) δ 152.0, 134.4, 130.4, 129.8, 129.7, 128.3, 123.1, 118.8, 115.2, 56.8, 45.4, 44.6, 44.5, 40.3. (ESI) m/z calcd for $C_{16}H_{23}N_3O_2$ ([M+H]$^+$) 322.1505, found 322.1690.

(3) *N*-2-Dimethylaminoethyl-5-dimethylamino-naphthalene-1-sulfonamide (43 mg, 0.13 mmol) was added to MeCN (10 mL) followed by addition of iodomethane (8.3 μL, 0.13 mmol). The reaction was stirred for 24 h and then the solvent was removed in vacuo to give guest **9** as a yellow oil. This oil was sonicated in chloroform (2 mL), and the residual solids were filtered and dried to give product as a light-yellow solid (10 mg, 16%). ^{1}H NMR (400 MHz; D_2O) δ 8.56 (d, J = 8.6 Hz, 1H), 8.31 (d, J = 7.4 Hz, 1H), 8.28 (d, J = 8.7 Hz, 1H), 7.75 (dd, J = 8.7, 8.6 Hz, 1H), 7.73 (dd, J = 7.7, 7.4 Hz, 1H), 7.46 (d, J = 7.7 Hz, 1H), 3.40 (m, 4 H), 3.09 (s, 9H), 2.90 (s, 6H). (ESI) m/z calcd for $C_8H_{12}N_2O_2$ (M$^+$) 336.1735, found 336.1751

Surface Characterization. *Preparation of Cavitand **3** Self-Assembled Monolayer (SAM).* A gold disk electrode (CH Instruments Inc., 2.0 mm in diameter) was abraded with fine silicon carbide paper and polished carefully with 0.3 and 0.05 μm alumina slurry and then sonicated in water. The cavitand **3** self-assembled monolayer was prepared by immersing the cleaned gold electrode in a 0.5 mM butanol solution of cavitand **3** for 5 h, followed by washing with ethanol and distilled water.

*Establishing Complete Cavitand **3** SAM with Space-Filling Molecules.* *N*-Octadecanethiol (ODT) and 11-mercaptoundecanoic acid (MUA) were chosen to fill the defects in the SAM left by cavitand absorption and mixed with cavitand **3** in butanol solution with molar ratio 10:1 (5 mM ODT or MUA, 0.5 mM **3**), respectively. SPR gold chips were fabricated with a 2 nm thick chromium adhesion layer, followed by deposition of a 46 nm thick gold layer via e-beam evaporation onto cleaned BK-7 glass slides. To prepare the mixed SAM of **3** and thiols ODT/MUA, gold substrates were immersed in the above butanol solution for 5 h, followed by washing with ethanol and distilled water.

Electrochemical Measurements. Cyclic voltammetric experiments were performed on a CHI 650A Electrochemical Workstation (CH Instruments Inc.). All experiments were carried out using a conventional three-electrode system with the gold disk electrode as working, a platinum foil as auxiliary, and a saturated calomel electrode as reference electrodes. The redox solution consisted of 25 mM aqueous KCl containing 2.5 mM $[Fe(CN)_6]^{3-}$ with a scan rate of 100 mV/s.

SPR Analysis of Guest Binding on SAMs. A dual channel SPR spectrometer NanoSPR-321 (NanoSPR, Addison, IL) with a GaAs semiconductor laser light source (λ = 670 nm) was used for all SPR measurements. The device comes with a high-refractive index prism (n = 1.61) and 30 μL flow cell. Surface interaction and modification were monitored using the angular scanning mode around the minimum angle. The modified gold substrate was clamped to a flow cell on a prism. An aqueous solution of **4** (5 mM) was injected into the flow cell and incubated for 30 min to allow guest binding to **3**. In each case, a 20 min rinse was performed before analysis of the resonance angle change, to ensure the removal of all nonspecifically bound guest molecules.

Protein binding of the cavitand:guest construct was measured similarly. A 2 mM aqueous solution of biotin guest **5** was injected into the flow cell and incubated on the 10:1 MUA:Cavitand **3** SAM gold substrate for 30 min followed by nanopure water rinsing. An aqueous solution of streptavidin (0.25 mg/mL) was injected into the flowcell, and the change in resonance angle recorded. The experiment was repeated on a blank MUA SAM, and the change in resonance angle upon streptavidin injection compared to that in the presence of **3**.

Fluorescence Microscopy Characterization. After the 10:1 MUA:**3** SAM gold substrate was incubated with 5 mM **4** and rinsed with nanopure water, fluorescence microscopy was carried out on a Zeiss LSM 510 confocal laser scanning microscope with 488 nm argon laser excitation and a CCD camera. Weak signal was observed due to fluorescence quenching from the gold surface.

Array Construction and SPR Imaging Characterization. A polydimethylsiloxane (PDMS) chip was prepared by mixing 10:1 prepolymer and curing agent and degassed for 20 min. The mixed solution was poured to a Petri dish and incubated at 70 °C in an oven for 1 h. The resultant PDMS chip was carefully peeled off and drilled with a homemade tool to generate a 2 × 2 array. PDMS array was tightly pressed on a plasmon cleaned gold substrate. After annealing in an oven at 70 °C for 20 min, a butanol solution of 10:1 MUA:**3** was pipetted on array cavities and incubated for 3 h. The solution was added several times during incubation to replenish solvent loss due to evaporation. After the deposition, the array was patted dry with a Kimwipe and rinsed with ethanol. The PDMS array chip was peeled off and the gold substrate was immersed in a 5 mM solution of **4**. After rinsing with nanopure water, the array was subjected to SPR imaging characterization.

The prepared array was mounted on an optical stage with a flow cell for SPR imaging. A red light emitting diode (LED, 648 nm) was used for excitation and the reflected images were captured by a cooled 12-bit CCD camera (Retiga 1300 from QImaging) with a resolution of 1.3 MP (1280 × 1024 pixels) and 6.7 μm × 6.7 μm pixel size.[25] The guest binding on the substrate surface was monitored by measuring changes in the reflectivity, and real time images were recorded.

RESULTS AND DISCUSSION

The synthesis of the target cavitand **3** is shown in Figure 1. Facile adsorption on a gold surface requires the presence of thiol or sulfide groups on the receptor, and obviously these should be incorporated at the base (or "feet") of the receptor. Introduction of thiols or thioacetates from known cavitands with alcohol feet proved problematic, so we turned to a precedented method of resorcinarene derivatization, by reacting a suitable thiol with alkene groups at the resorcinarene base.[22] Olefinic resorcinarene **1** was converted to the octamide cavitand **2** in 29% overall yield (3 steps) by reaction with excess 1,2-difluoro-4,5-dinitrobenzene, followed by $SnCl_2$/HCl reduction and acylation under Schotten-Baumann conditions.[17] It should be noted that the terminal olefins are stable to these reduction conditions, although other reported reductions (e.g., Raney Nickel/H_2) are unsuitable. The addition of thiol groups was performed after this stage as the sulfide function does not survive the harsh reduction conditions necessary for synthesis of octamide **2**. Hydroboration of the olefins in **2** with 9-BBN in the presence of 1-decanethiol proceeded smoothly, furnishing the target sulfide-footed cavitand **3** in 79% yield after column chromatography. As expected, introduction of the sulfide feet has no effect on the folding properties of **3**; a stable vase-like structure was observed by ^{1}H NMR analysis in nonpolar solvents (see the Supporting Information). The cavitand is soluble in a wide variety of organic solvents (although not water), and *n*-butanol was chosen as a suitable solvent for surface deposition to limit damage to the cleaned surface while allowing sufficiently slow evaporation for clean surface formation. In order to allow real-time SPR spectroscopy analysis of the system, gold-plated electrodes were chosen as the target surface. SPR is a surface analysis method based on detecting refractive index changes due to the adsorption or noncovalent recognition of target molecules, and is useful for monitoring affinity interactions in real-time without the use of a label.

The receptor was deposited onto the cleaned chip by immersing the cleaned gold electrode in a 0.5 mM solution of cavitand **3** in *n*-butanol for 5 h, followed by rinsing and drying. Electrochemical analysis was used to determine the successful adsorption of **3** on the surface. Figure 2 shows the cyclic voltammograms of the bare and modified electrodes in 25 mM KCl solution containing 2.5 mM $[Fe(CN)_6]^{3-}$ as charge carrier. Well-defined redox peaks were observed for the facile probe of $[Fe(CN)_6]^{3-/4-}$ on a bare surface. The presence of cavitand **3** caused a 63% decrease in current, indicating an impeded electrochemical reaction at the electrode surface. The increase in peak separation, ΔE_p, from 90 to 194 mV, further points to a blocked process when the thiocavitand was assembled on the surface. The retention of some signal in the cyclic voltammogram, however, indicates that simple adsorption of the sulfide cavitand **3** did not cause complete coverage of the plate. The flexible cavitand **3** did not form a fully packed self-assembled monolayer, most likely due to poorly favorable interactions between cavitands at the surface. There are two possible

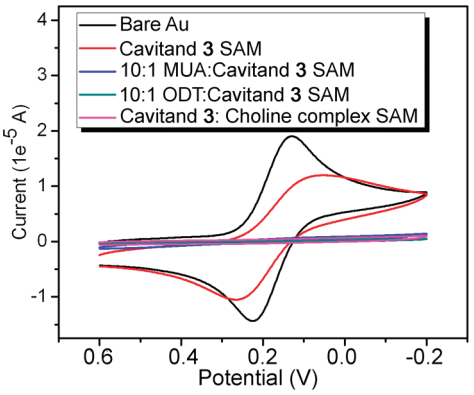

Figure 2. Cyclic voltammetry characterization of various surface coverages; charge carrier 2.5 mM $K_3Fe(CN)_6$ in 25 mM KCl at 100 mV/s.

conformations of the octamide cavitand, the folded "vase" conformation seen in Figure 1, and a flattened "kite" conformation with no cavity. This kite conformation is disfavored in aprotic solvents, as the cavitand is held in the desired "vase" conformation by the seam of hydrogen bonding amides at the rim. This seam is disrupted in protic solvents such as butanol, and the host undergoes rapid equilibration between the folded vase form and the unfolded kite conformation.[26,27] Figure 3 shows a cartoon representation of the process.

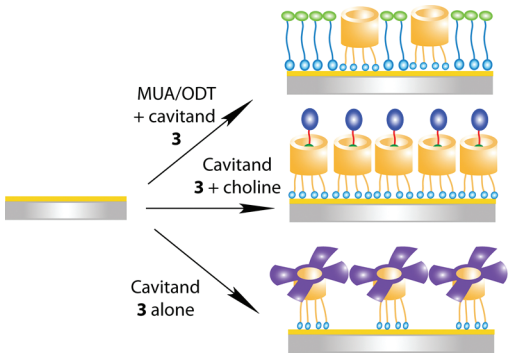

Figure 3. Illustration of cavitand **3** adsorption on the surface in the presence of (a) space-filling molecules MUA or ODT, (b) choline chloride, and (c) no additive.

To corroborate the theory that unfolded conformations of **3** are responsible for the incomplete coverage, the deposition experiment was performed in the presence of a good guest molecule. Strongly bound species such as tetramethylammonium cations or choline have been shown to template the self-assembly of amide-based cavitands in protic or aqueous solution and favor the "vase" conformation.[28] Choline chloride (5 mM) was added to the 0.5 mM solution of **3**, and deposited on the cleaned gold electrode as before. After rinsing, the cyclic voltammogram was recorded (Figure 2). In the presence of strong guest, no signal was observed in the CV, indicating formation of a SAM that completely shuts down the electronic communication due to a packed surface structure.

Unfortunately, while adsorption of the cavitand was successful in the presence of a strong guest, the presence of choline in the system removes the possibility of directed guest binding by the cavitand at the gold surface, as the cavity of **3** is filled. An alternate possibility is to "fill the gaps" with a suitable

dx.doi.org/10.1021/la2039398 | *Langmuir* 2012, 28, 1391−1398

space-filling molecule that has no cavity. Even though a close-packed monolayer of empty cavitand **3** was inaccessible, the spaces between receptors need not be filled with other receptor molecules, but rather with simple molecules whose sole task is to fill the remaining defects in the monolayer. To prevent unwanted interactions between added guests and defects in the monolayer, films were also made by adsorbing a mixture of **3** and long chain aliphatic thiols. Two thiols were tested, hydrophobic *N*-octadecanethiol (ODT) and hydrophilic 11-mercaptoundecanoic acid (MUA), where the narrow alkanethiols can fill in gaps in the monolayer (Figure 3). Formation of the mixed monolayers was performed using the same method of cavitand adsorption. The gold chips were immersed in a 10:1 mixture of **3** and the requisite thiol as before, and surface coverage was determined by cyclic voltammetry. Both thiols were successful in forming a fully packed monolayer. In each case, no signal was observed in the voltammogram, indicating formation of a SAM that effectively shuts down the electron communication due to a packed surface structure. The CV data does not reveal whether mixed monolayers were formed or whether embedded cavitands were still functional, however, and this was determined by analysis of guest binding.

Guest Recognition. Having incorporated the host on the gold surface, the unanswered question was whether the cavitands retained their guest binding properties. Guest binding could be limited by unfolded conformations of cavitand in the **3** monolayer (in the absence of choline template), and MUA or ODT could outcompete **3** in surface adsorption, leading to zero cavitand at the **3**:ODT or **3**:MUA surface. The guest recognition properties of the three surfaces were established by monitoring the recognition event with guest molecules in real time by SPR analysis. The hosts are open-ended, and are well-precedented to bind substituted trimethylammonium (NMe_3^+) salts in both aprotic[18] and aqueous solvents.[16,23,29] The trimethylammonium tag acts as an anchor, and a variety of species can be displayed above the rim of the receptor.

The cavitand-adorned gold substrate was clamped down by a flow cell on a high-refractive index prism for SPR measurement, allowing exposure of the surface to aqueous medium. The flowcell apparatus allowed the simple introduction of suitable guest molecules by injection of targets in aqueous solution. Cavitand **3** displays a hydrophobic cavity to the aqueous milieu above the surface, capable of binding suitably sized guests through hydrophobic and cation−π interactions. To this end, we utilized a series of guests **4**−**9** that had been previously shown to bind in a membrane-bound deep cavitand in aqueous solution,[23] as shown in Figure 1. To allow for multiple analysis methods, NMe_3^+-tagged fluorescein **4** was selected as the initial test subject.

An aqueous solution (5 mM) of guest **4** was injected into the chip-containing flow cell and incubated for 30 min to allow complete guest binding to **3**, followed by an aqueous rinsing process to remove the unincorporated excess. Initially, the cavitand **3** SAM and the **3**:ODT surfaces were exposed to guest, along with a control surface of ODT alone (Figure 4). The change in resonance angle upon treatment of the three derivatized surfaces is shown in Figure 5. An increase in resonance angle of 0.40° is observed upon addition of guest to the cavitand **3** SAM, indicating absorption of guest **4** to the surface. The signal increase persists after washing, and **4** has no affinity for the bare gold surface itself. The absorbed guests are held in place by hydrophobic and cation-π interaction with the cavity of **3**, and the fluorescein tag is displayed above the cavitand at the surface.

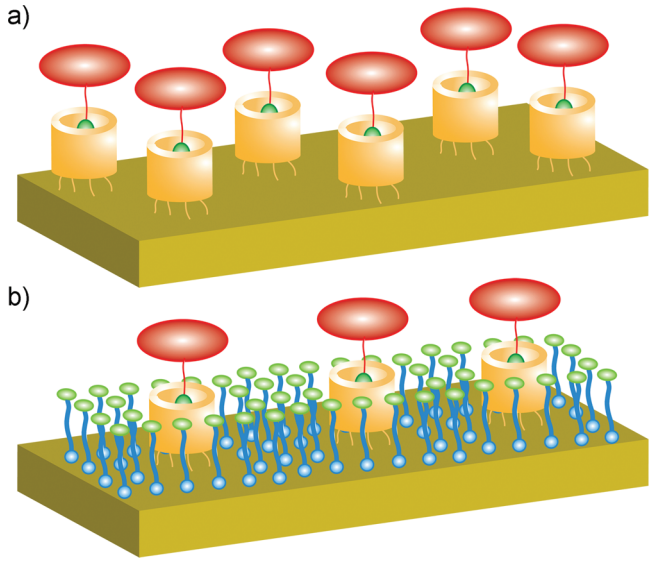

Figure 4. Representation of the experiment: (a) Thiocavitand-SAM with bound substrate. (b) Mixed MUA-thiocavitand SAM indicating guest binding.

While the surface-adsorbed **3** retains its solution-phase binding properties, the efficacy of the space-filling strategy was undetermined. An aqueous solution of guest **4** was exposed to the chip containing the hydrophobic **3**:ODT mixed SAM. When **4** was exposed to the **3**:ODT mixed SAM, a smaller change in resonance angle (0.27°) occurred than for that of **3** alone,. This indicates adsorption of the guest to the SAM, and the smaller signal would be expected for a surface with a lower concentration of host **3**. Unfortunately, significant background absorption was observed in the ODT monolayer. The SPR signal increase upon addition of **4** is similar (0.26°) for a single ODT monolayer as the signal increase for the 10:1 ODT-**3** mix. Two possibilities present themselves: either ODT outcompeted **3** for surface attachment, or the affinity of **4** for the ODT monolayer itself is too high. While guest **4** is charged and water-soluble, it is still quite lipophilic, and significant absorption occurs at the hydrophobic SAM chains.

To suppress the background absorption, the more hydrophilic 11-mercaptoundecanoic acid (MUA) was used as filler. The carboxylic acid groups are oriented toward the aqueous medium, lowering the lipophilicity of the SAM and limiting the background absorption due to nonspecific hydrophobic adsorption. A self-assembled monolayer of MUA was constructed, and the affinity of guest **4** for MUA itself was determined. Upon treatment of the MUA SAM with an aqueous solution of guest **4**, a negligible SPR signal increase (0.04°) was observed, indicating minimal affinity of guest **4** for the surface. When guest **4** was exposed to the 10:1 **3**:MUA SAM, however, a strong signal increase was observed (0.16°).

Deep cavitands such as **3** show a wide scope of guest binding in solution, but this is lessened significantly in competitive solvents (i.e., those that can fill the cavity) and aqueous solution. At the surface, another challenge arises - the guest must be of suitable size and hydrophobicity to cause a sufficiently large refractive index change for effective detection in the SPR experiment. To analyze the range of species that could detected in the system, we generally focused on water-

dx.doi.org/10.1021/la2039398 | *Langmuir* 2012, 28, 1391−1398

	Cav **3**	ODT	1:10 Cav **3**:ODT	Cav **3**	MUA	1:10 Cav **3**:MUA
ΔΘ (Guest **4**)	0.40 (±0.06)	0.26 (±0.02)	0.27 (±0.01)	0.40 (±0.06)	0.04 (±0.01)	0.16 (±0.03)

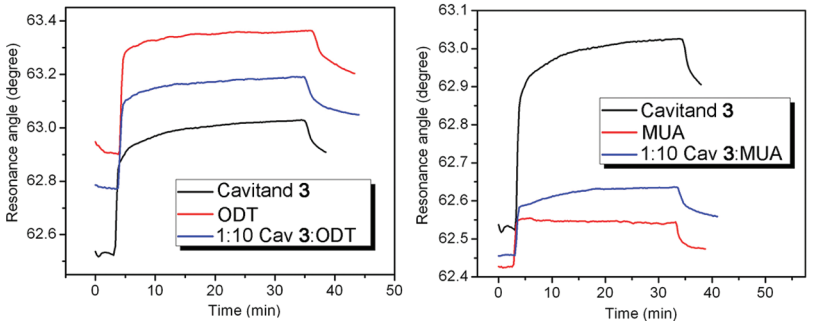

Figure 5. Sensorgrams showing the SPR response upon addition of guest **4** to the representative surfaces.

soluble guests of varying sizes with trimethylammonium anchors. The guests are shown in Figure 1 and were all injected into the system as 5 mM aqueous solutions. As would be expected, all guests **5**–**9** showed smaller signal SPR increases upon binding in the **3**:MUA monolayer than fluorescein guest **4** due to their smaller size (Table 1). The

Table 1. Resonance Angle Change upon Guest Binding

guest	4	5	6	7	8	9
Θ (3:MUA;1:10)	0.16	0.04	0	0.02	0.05	0.06
Θ (MUA)	0.04	0.01	0	0	0.02	0.02

binding of adamantanol **6** was not observed by SPR, but the reason for this is unclear, as adamantyl groups are well-precedented guests for octamide cavitands in solution.[10] Interestingly, the observed binding for cetyltrimethylammonium iodide was poor; the highly hydrophobic alkyl chains should cause significant resonance angle change upon binding, but little was observed. This is most likely due to the unfavorability of guest binding; the hydrophobic penalty upon display of the C_{16} chains to the aqueous medium outweighs any enthalpic benefit from NMe_3^+ binding in the cavity. Changes in resonance angle were observed upon binding of other, less hydrophobic NMe_3^+-tagged guests **5** and **7**–**9**. All four guests were immobilized at the surface and the signal increase was concomitant with the size of the headgroup. The changes in resonance angle are small, but reproducible, and only minimal background signal change was observed, indicating the selectivity of the system for suitably tagged targets. The raw SPR sensorgrams are provided in the Supporting Information. Attempts were made to corroborate the SPR experiment using fluorescence microscopy. The fluorescent guest **4** was used for this analysis, but unfortunately the fluorophore exhibited significant quenching from the gold surface, and only very weak signal was observed in the experiment.

SPR Imaging Analysis of Cavitand Arrays. The simple adhesion of cavitand **3** at the surface suggested the possibility of forming defined arrays of cavitand on the gold surface. Microarrays have been proposed as powerful tools for routine screening and high-throughput tests in medical and biological fields. On account of their scalable and cost-effective fabrication, microarray resonators are particularly well-suited for multiplexed diagnostic applications. We applied the self-assembly of the cavitand **3**: guest interaction based on the microarray format, which provides spatial information on a sensing chip for binding sites as well quantitative assessment of the interaction. The application of a microarray-based technique in studying cavitand-guest interaction holds great promises for parallel evaluation of affinity for various guests and opens the door to large-scale screening of targets in the fields of drug discovery and pharmaceutics.

Implementation of these analytical tools often relies on signal amplification strategies to reach the satisfied sensitivity levels. Fluorescence-based readout systems are by far the most widespread. However, common fluorescence-based microarray requires preliminary attachment of a quantifiable fluorescent tag and has limited application for online detection, not to mention the quenching we observed in our preliminary experiments (vide infra). We therefore turned to SPR imaging (SPRi) for array analysis. SPRi retains the high sensitivity of label free SPR measurement while providing spatial information of a sensing surface suitable for microarray detection. SPRi measures the intensity change of the reflective light at a fixed angle, and the image of the entire biochip can be recorded with high spatial resolution in real time.[30] Coupled with microarray-based techniques, multiple microRNA sequences have been detected at low concentrations,[31] and rapid detection of relevant protein biomarkers and nucleic acids is possible by combining SPRi and enzymatic reaction amplification.[32] Beside nucleic acids, lectin-carbohydrate interactions[33]and lipid–protein interactions were also studied via SPRi on bilayer lipid membrane arrays from photolithography[34] and PDMS microchips.[35]

In order to prepare the array of host molecules on the surface, a PDMS stamp was prepared. A butanol solution of 10:1 MUA:**3** was pipetted onto the array cavities. Butanol was chosen as solvent to limit overly rapid evaporation during deposition of the cavitand:MUA array as before; ethanol was unsuitable for this reason, and hydrocarbon solvents suffered from leakage from the PDMS stamp. SPR imaging of these arrays requires a significant change in resonance angle for suitable sensitivity. Upon formation of the **3**:MUA monolayer, only minimal changes in signal were observed between array and background. As SPR spectroscopy is effective for detecting guest binding, we attempted to attain SPR image data on the host:guest complex rather than the **3**:MUA monolayer alone. The preformed array was incubated with a 5 mM aqueous solution of fluorescent guest **4** for 30 min at ambient temperature, and the chip exposed to SPR imaging characterization. In this case, the resolution of the cavitand:**4** host guest complex was sufficient for good SPR imaging analysis.

dx.doi.org/10.1021/la2039398 | *Langmuir* 2012, 28, 1391–1398

Imaging of the array is shown in Figure 6. An increase in reflected light intensity was observed upon binding of guest **4**

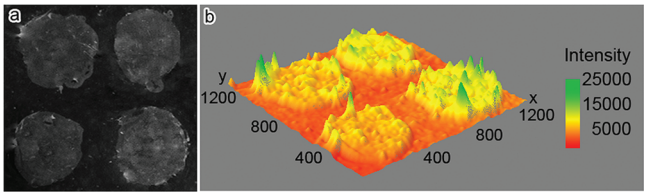

Figure 6. (a) SPR imaging of fluorescent guest **4** incubated on a 2 × 2 array of cavitand **3** (4 mm in diameter); (b) corresponding intensity 3D profile.

that only occurred in the 2 × 2 array. Figure 6 shows two views of the array, a plan view of the light/dark profile (Figure 6a), and a 3D profile indicating signal intensity (Figure 6b) that gives better spatial resolution. The gold chip was plasma cleaned before use and remained hydrophilic after removal of the PDMS stamp, and therefore provided little nonspecific adsorption for fluorescent guest **4** outside the array boundary. This data shows that not only is the sulfide-footed cavitand **3** amenable to surface deposition, it is possible for defined arrays of the system. The guest binding properties can be determined in a label-free manner in mild conditions; although fluorescein-derived guest **4** was used for this purpose, the detection is not based upon fluorescence. Any NMe_3^+-tagged guest of suitable size is amenable to this process.

Protein Recognition. The cavitand monolayer has excellent substrate selectivity: suitable targets are substituted NMe_3^+ ions. In order to widen the scope of the system, tagged guests that themselves contain a recognition element are desired. Extended cap-biotin guest **5** can be attached to the surface by interaction of the trimethylammonium tag with cavitand **3**, and the biotin group displayed above the surface for immobilization of biomolecules. Sequential injection of guest and streptavidin protein allows monitoring of the biosensing power of the system.

The **3**:MUA surface was utilized for this experiment. After immersion of the gold chip in a 10:1 solution of MUA:**3** followed by rinsing with butanol and water, the modified gold substrate was dried under a N_2 stream and clamped to a flow cell on an SPR prism. A 2 mM aqueous solution of cap-biotin guest **5** was injected into the flow cell and monitored by SPR analysis. Upon binding of **5**, a change in resonance angle of 0.039° was observed (Figure 7). Subsequent addition of a 0.25 mg/mL solution of streptavidin caused an increase in resonance angle of 0.14°, indicating the immobilization of the streptavidin protein at the surface. In the absence of the biotinylated guest **5** (Figure 7b), minimal signal increase was observed. In addition, no signal was observed in the absence of cavitand (i.e., the MUA monolayer alone), indicating that the neither the guest nor the protein can be immobilized by MUA alone, and the biosensing process requires the specific noncovalent interaction of the cavitand: biotin guest: streptavidin complex.

CONCLUSIONS

This work has shown the first use of a self-folding deep cavitand on a gold surface. By incorporating sulfide feet at the base of an octamide deep cavitand, surface attachment has been achieved. The attachment process can be studied by electrochemical and SPR methods. Complete monolayer formation is not observed

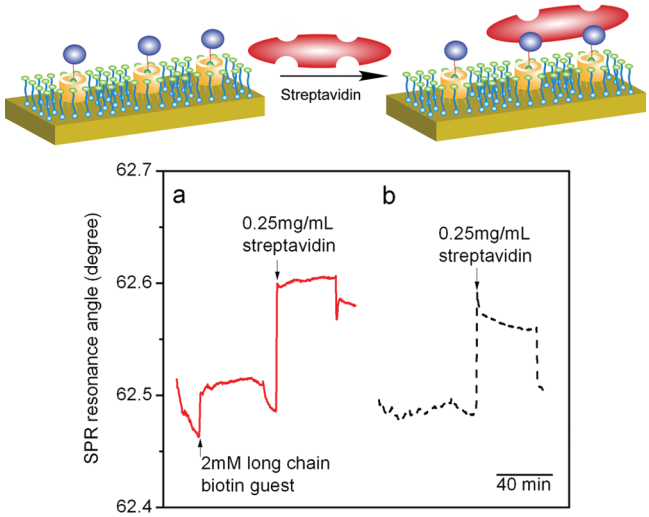

Figure 7. SPR sensorgram of streptavidin incubated with 10:1 MUA:Cavitand **3** SAM Au substrate in the presence (a) and absence (b) of biotinylated guest **5**.

from protic solvents due to the conformational flexibility of the host, however this can be circumvented either by performing the adsorption experiment in the presence of a template such as choline chloride that provides rigidity to the cavitand through host:guest interactions, or by addition of space-filling thiols to cover any gaps in the cavitand adsorption layer. The cavitand is capable of binding trimethylammonium-tagged guests from an aqueous medium, and the binding event can be monitored by surface plasmon resonance techniques. While the guest must protrude into the solvent for adequate detection, groups as small as a benzene ring can be detected by this method. The host can be deposited in 2 × 2 microarrays on the surface, and the binding of suitable guests allows detection of these arrays by SPR imaging techniques. When biotin-labeled guests are used, the cavitand:guest construct can recognize and immobilize streptavidin proteins from aqueous solution, acting as a fully synthetic biosensor. Further work on the biosensing properties of this system is underway in our laboratory.

ASSOCIATED CONTENT

Supporting Information

NMR spectra and SPR sensorgrams not included in the text. This material is available free of charge via the Internet at http://pubs.acs.org.

AUTHOR INFORMATION

Corresponding Author

*E-mail: jrebek@scripps.edu; quan.cheng@ucr.edu; richard.hooley@ucr.edu.

ACKNOWLEDGMENTS

Acknowledgment is made by R.J.H. to the donors of the American Chemical Society Petroleum Research Fund for support of this research. Q.C. acknowledges financial support from NSF (CHE-1059050). J.R. acknowledges financial support from NSF (CHE-1037590).

REFERENCES

(1) (a) Daly, S. M.; Grassi, M.; Shenoy, S. K.; Ugozzoli, F.; Dalcanale, E. *J. Mater. Chem.* **2007**, *17*, 1809−1818. (b) Schierbaum, K. D.;

Weiss, T.; Thoden van Velzen, E. U.; Engbersen, J. F. J.; Reinhoudt, D. N.; Göpel, W. *Science* **1994**, *265*, 1413−1415. (c) Thoden van Velzen, E. U.; Engbersen, J. F. J.; de Lange, P. J.; Mahy, J. W. G.; Reinhoudt, D. N. *J. Am. Chem. Soc.* **1995**, *117*, 6853−6862. (d) Thoden van Velzen, E. U.; Engbersen, J. F. J.; Reinhoudt, D. N. *J. Am. Chem. Soc.* **1994**, *116*, 3597−3598.
(2) (a) Menozzi, E.; Pinalli, R.; Speets, E. A.; Ravoo, B. J.; Dalcanale, E.; Reinhoudt, D. N. *Chem.—Eur. J.* **2004**, *10*, 2199−2206. (b) Corbellini, F.; Mulder, A.; Sartori, A.; Ludden, M. J. W.; Casnati, A.; Ungaro, R.; Huskens, J.; Crego-Halama, M.; Reinhoudt, D. N. *J. Am. Chem. Soc.* **2004**, *126*, 17050−17058.
(3) Zyryanov, G. V.; Kang, Y.; Rudkevich, D. M. *J. Am. Chem. Soc.* **2003**, *125*, 2997.
(4) Guerrini, L.; Garcia-Ramos, J. V.; Domingo, C.; Sanchez-Cortes. *Anal. Chem.* **2009**, *81*, 1418−1425.
(5) Nikolelis, D. P.; Petropoulou, S. S. E.; Theoharis, G. *Electroanalysis* **2003**, *15*, 1616−1624.
(6) (a) Pinalli, R.; Nachtigall, F. F.; Ugozzoli, F.; Dalcanale, E. *Angew. Chem., Int. Ed.* **1999**, *38*, 2377−2380. (b) Suman, M.; Freddi, M.; Massera, C.; Ugozzoli, F.; Dalcanale, E. *J. Am. Chem. Soc.* **2003**, *125*, 12068−12069. (c) Melegari, M.; Suman, M.; Pirondini, L.; Moiani, D.; Massera, C.; Ugozzoli, F.; Kalenius, E.; Vainiotalo, P.; Mulatier, J.-C.; Dutasta, J.-P.; Dalcanale, E. *Chem.—Eur. J.* **2008**, *14*, 5772−5779. (d) Pirondini, L.; Dalcanale, E. *Chem. Soc. Rev.* **2007**, *36*, 695−706. (e) Maffei, F.; Betti, P.; Genovese, D.; Montalti, M.; Prodi, L.; De Zorzi, R.; Geremia, S.; Dalcanale, E. *Angew. Chem., Int. Ed.* **2011**, *50*, 4654−4657.
(7) Ludden, M. J. W.; Reinhoudt, D. N.; Huskens, J. *Chem. Soc. Rev.* **2006**, *35*, 1122−1134.
(8) (a) Xu, H.; Ling, X. Y.; van Bennekom, J.; Duan, X.; Ludden, M. J. W.; Reinhoudt, D. N.; Wessling, M.; Lammertink, R. G. H.; Huskens, J. *J. Am. Chem. Soc.* **2009**, *131*, 797−803. (b) Ludden, M. J. W.; Li, X.; Greve, J.; van Amerongen, A.; Escalante, M.; Subramaniam, V.; Reinhoudt, D. N.; Huskens, J. *J. Am. Chem. Soc.* **2008**, *130*, 6964−6973.
(9) (a) Ludden, M. J. W.; Reinhoudt, D. N.; Huskens, J. *Small* **2006**, *2*, 1192−1202. (b) Ludden, M. J. W.; Mulder, A.; Tampe, R.; Reinhoudt, D. N.; Huskens, J. *Angew. Chem., Int. Ed.* **2007**, *46*, 4104−4107.
(10) Hooley, R. J.; Rebek, J. Jr. *Chem. Biol.* **2009**, *16*, 255−264.
(11) Cram, D. J. *Container Molecules and their Guests*; Royal Society of Chemistry: Cambridge, U.K., 1994.
(12) Moran, J.; Ericson, J.; Dalcanale, E.; Bryant, J.; Knobler, C.; Cram, D. *J. Am. Chem. Soc.* **1991**, *113*, 5707−5714.
(13) Rudkevich, D. M.; Hilmersson, G.; Rebek, J. Jr. *J. Am. Chem. Soc.* **1997**, *119*, 9911−9912.
(14) Far, A. R.; Shivanyuk, A.; Rebek, J. Jr. *J. Am. Chem. Soc.* **2002**, *124*, 2854−2855.
(15) Hof, F.; Trembleau, L.; Ullrich, E. C.; Rebek, J. *Angew. Chem., Int. Ed.* **2003**, *42*, 3150−3153.
(16) Biros, S. M.; Ullrich, E. C.; Hof, F.; Trembleau, L.; Rebek, J. *J. Am. Chem. Soc.* **2004**, *126*, 2870−2876.
(17) Rudkevich, D. M.; Hilmersson, G.; J. Rebek, J. Jr. *J. Am. Chem. Soc.* **1998**, *120*, 12216−12225.
(18) Purse, B. W.; Ballester, P.; Rebek, J. Jr. *J. Am. Chem. Soc.* **2003**, *125*, 14682−14683.
(19) Purse, B. W.; Rebek, J. Jr. *Proc. Natl. Acad. Sci., U.S.A.* **2005**, *102*, 10777−10782.
(20) Iwasawa, T.; Hooley, R. J.; Rebek, J. Jr. *Science* **2007**, *317*, 493−496.
(21) Hooley, R. J.; Iwasawa, T.; Rebek, J. Jr. *J. Am. Chem. Soc.* **2007**, *129*, 15330−15339.
(22) van Velzen, E. U. T.; Engbersen, J. F. J.; Renhoudt, D. N. *Synthesis* **1995**, 989−997.
(23) Liu, Y.; Liao, P.; Cheng, Q.; Hooley, R. J. *J. Am. Chem. Soc.* **2010**, *132*, 10383−10390.
(24) Poe, S. L.; Bogdan, A. R.; Mason, B. P.; Steinbacher, J. L.; Opalka, S. M.; McQuade, D. T. *J. Org. Chem.* **2009**, *74*, 1574−1580.
(25) Wilkop, T.; Wang, Z.; Cheng, Q. *Langmuir* **2004**, *20*, 11141−11148.
(26) Haino, T.; Rudkevich, D. M.; Rebek, J. Jr. *J. Am. Chem. Soc.* **1999**, *121*, 11253−11254.
(27) Cram, D. J.; Choi, H. J.; Bryant, J. A.; Knobler, C. B. *J. Am. Chem. Soc.* **1992**, *114*, 7748−7765.
(28) Butterfield, S. M.; Rebek, J. Jr. *J. Am. Chem. Soc.* **2006**, *128*, 15366−15367.
(29) Kim, Y. J.; Lek, M. T.; Schramm, M. P. *Chem. Commun.* **2011**, *47*, 9636−9638.
(30) Scarano, S.; Mascini, M.; Turner, A.; Minunni, M. *Biosens. Bioelectron.* **2010**, *25*, 957−966.
(31) Zhou, W.; Chen, Y.; Corn, R. M. *Anal. Chem.* **2011**, *83*, 3897−3902.
(32) Seefeld, T. H.; Zhou, W.; Corn, R. M. *Langmuir* **2011**, *27*, 6534−6540.
(33) Linman, M. J.; Yu, H.; Chen, X.; Cheng, Q. *ACS Appl. Mater. Interfaces* **2009**, *8*, 1755−1762.
(34) Wang, Z.; Wilkop, T.; Han, J. H.; Dong, Y.; Linman, M. J.; Cheng, Q. *Anal. Chem.* **2008**, *80*, 6397−6404.
(35) Taylor, J. D.; Linman, M. J.; Wilkop, T.; Cheng, Q. *Anal. Chem.* **2009**, *81*, 1146−1153.